

How low-excitation, fine-structure atomic lines can help understand the chemical evolution of PPNe and PNe

M. Santander-García^{1,2}, V. Bujarrabal¹ & J. Alcolea¹

¹Observatorio Astronómico Nacional, Madrid, Spain

²Centro de Astrobiología CSIC-INTA, Madrid, Spain

e-mail: m.santander@oan.es

Abstract

The nebular gas composition evolves very strongly during the post-AGB/PPN phase, from the molecule-rich AGB shells to the fully ionized evolved PNe, which has important effects on the thermodynamics and dynamics of nebulae in the intermediates phases and on their observational properties. Before the end of its operational life, Herschel/HIFI provided us with very high-spectral resolution and sensitivity FIR observations of the C I, C II and O I emission of a sample of 10 C-rich and O-rich PPNe and young PNe, 2 AGB stars and 1 supergiant star. We derive estimates for the mass of the C I- and C II-rich emitting regions (which are located between the H II and molecular regions) of this sample. Results range between $\sim 10^{-4}$ and $\sim 10^{-2} M_{\odot}$ for the C I-emitting region, and between $\sim 10^{-5}$ and $\sim 0.26 M_{\odot}$ for the C II-emitting region. We also determine the characteristic excitation temperature of the C I-rich region and compare atomic and molecular line profiles in order to determine the spatial distribution of the atomic emission and the origin of dissociation of molecules which is mostly due to the stellar UV field, except in some young PNe which could also be affected by shocks.

The results of this preliminary study will be presented in more detail in a forthcoming paper (Santander-García et al., in preparation).

The sample

The sample observed with HERSCHEL/HIFI consists of

- 6 C-rich PPNe and young PNe (NGC 7027, The Red Rectangle, CRL 618, CRL 2688, NGC 6720, and IRAS 21282+5050)
- 4 O-rich PPNe and young PNe (NGC 6302, M1-92, M 2-9 and OH231.8+4.2)
- 2 AGB stars (CIT 6 and IK Tau)
- 1 supergiant (Betelgeuse).

Profile analysis

The C I and C II line profiles provide information on the kinematical distribution of their corresponding emitting regions. Information on the spatial distribution can be constrained via comparisons with CO line profiles from other works. Examples of preliminary analyses are shown in Figures 1 and 2.

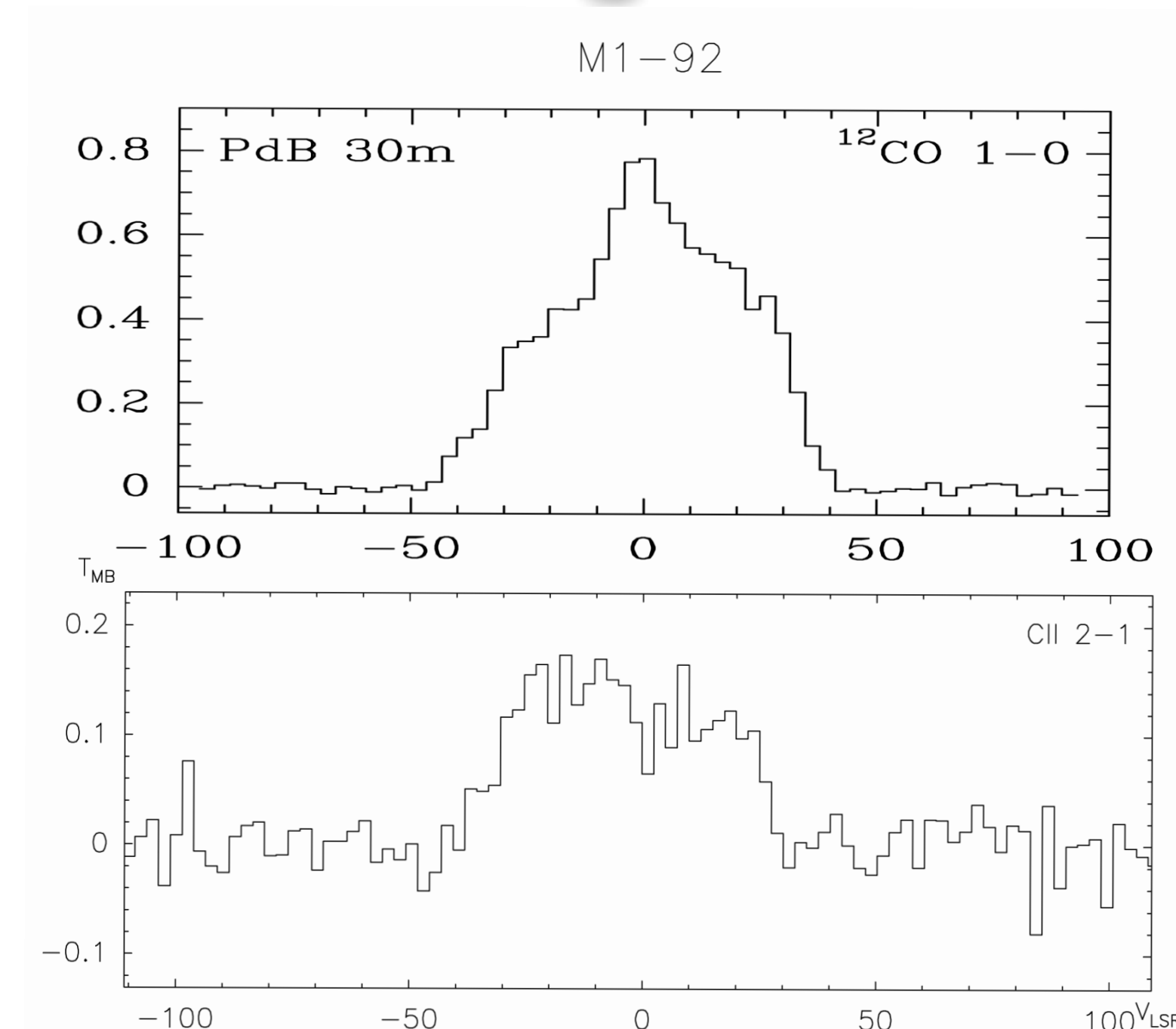


Figure 1. M1-92: C II emission shows a depression at low velocities, as opposed to CO emission (adapted from Bujarrabal et al., 1997, A&A, 320, 540), even at higher J . This absence of low velocities could be indicative of shocks. C I is not detected in this object. Both of these profiles show significantly lower velocities than the ionized bubble (INII). Solf 1994, A&A, 282, 567).

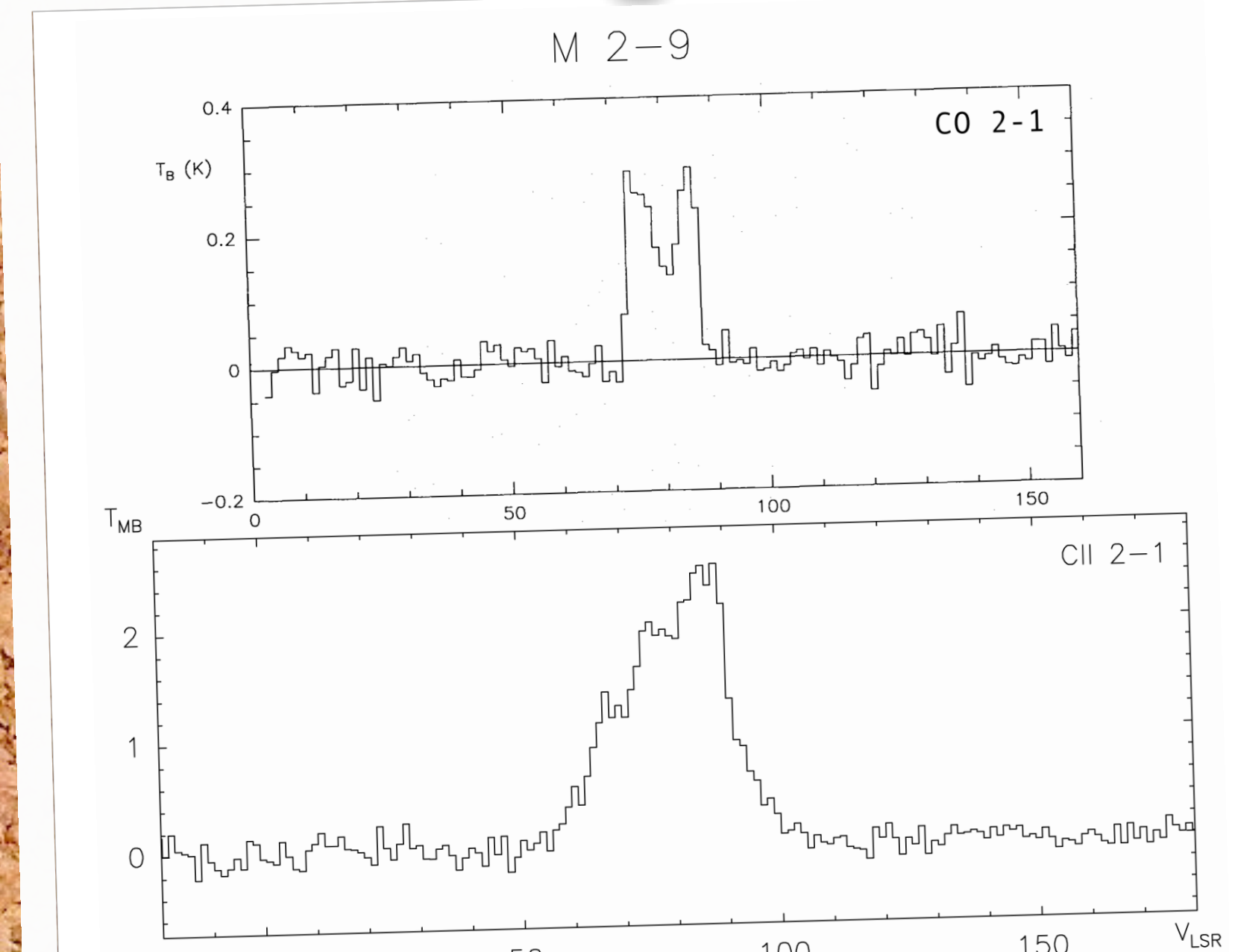


Figure 2. M 2-9: C II emission is broader than CO 2-1 emission and therefore reaches larger velocities, indicating a rapidly expanding PDR. Peaks do not clearly correspond to the expansion velocities of the equatorial circumnary disks (Castro-Carrizo et al. 2012, A&A, 545, 1). CO 2-1 line profile adapted from Bachiller et al. 1989, A&A, 227, 188. C I is not detected in this object.

Preliminary mass analysis

All our sources have been detected in C I and/or C II with the exception of OH231.8+4.2, which shows no signs of C I or C II emission with the achieved signal to noise (rms 7, 16 and 120 mK in the C I 1-0, 2-1 and C II 2-1 transitions respectively). The AGB stars IK Tau and CIT 6 show very dubious C I and C II emission and thus have been not included in this preliminary analysis.

We have first derived the excitation temperature T_{ex} from the relative intensities of the C I 1-0 and 2-1 transitions and the population levels, under the assumption that the emitter zone is small compared to the beam size (44 and 26 arcsec respectively). This T_{ex} is probably similar to the kinetic temperature T_k given the very low Einstein coefficients of these forbidden transitions. Next, we computed the mass of the C I-rich region from the derived excitation temperature and the flux of the 1-0 transition.

We also estimated the mass of the C II-rich region from the flux of the C II 2-1 transition, corrected for a factor taking into account the 12 arcsec beam in the cases where this size is comparable to the size of the photodissociation region (PDR). We also computed the characteristic density in order to check that additional correction factors were not necessary in any of the sources of the sample.

Preliminary results are listed in Table 1 along with the central star's T_{eff} and luminosity and the mass of the CO envelope obtained from the literature and corrected for the distance adopted for this work.

Object	T_{eff} (K)	L (L_{\odot})	T_{ex} (K)	$M_{\text{C I}}$ (M_{\odot})	$M_{\text{C II}}$ (M_{\odot})	M_{CO} (M_{\odot})
NGC 7027	200,000	10,700	55	2.7×10^{-2}	0.26	1.3
Red Rectangle	7,750	6,050	80	2.4×10^{-3}	8.7×10^{-4}	6.7×10^{-3}
CRL 2688	7,000	5,500	23	1.7×10^{-3}	2×10^{-5}	9.2×10^{-2}
NGC 6720	125,000	200	43	6.5×10^{-3}	!	
IRAS 21282+5050	30,000	2,400	54	3×10^{-2}	0.13	1.2
CRL 618	30,000	10,000	32	1.1×10^{-2}	1.3×10^{-3}	0.4
Betelgeuse	3,500	510,000	45	6.3×10^{-4}	4.6×10^{-5}	6.7×10^{-5}
NGC 6302	20,000	2,000	95	1.7×10^{-2}	0.12	0.14
M1-92	6,500	7,000	-	-	4.2×10^{-2}	1.3
M 2-9	25,000	1,700	-	-	3.5×10^{-2}	1.2×10^{-2}

Table 1. Relevant parameters of the selected sample.

‘!’ means uncertain; ‘-’ refers to a non-detection.

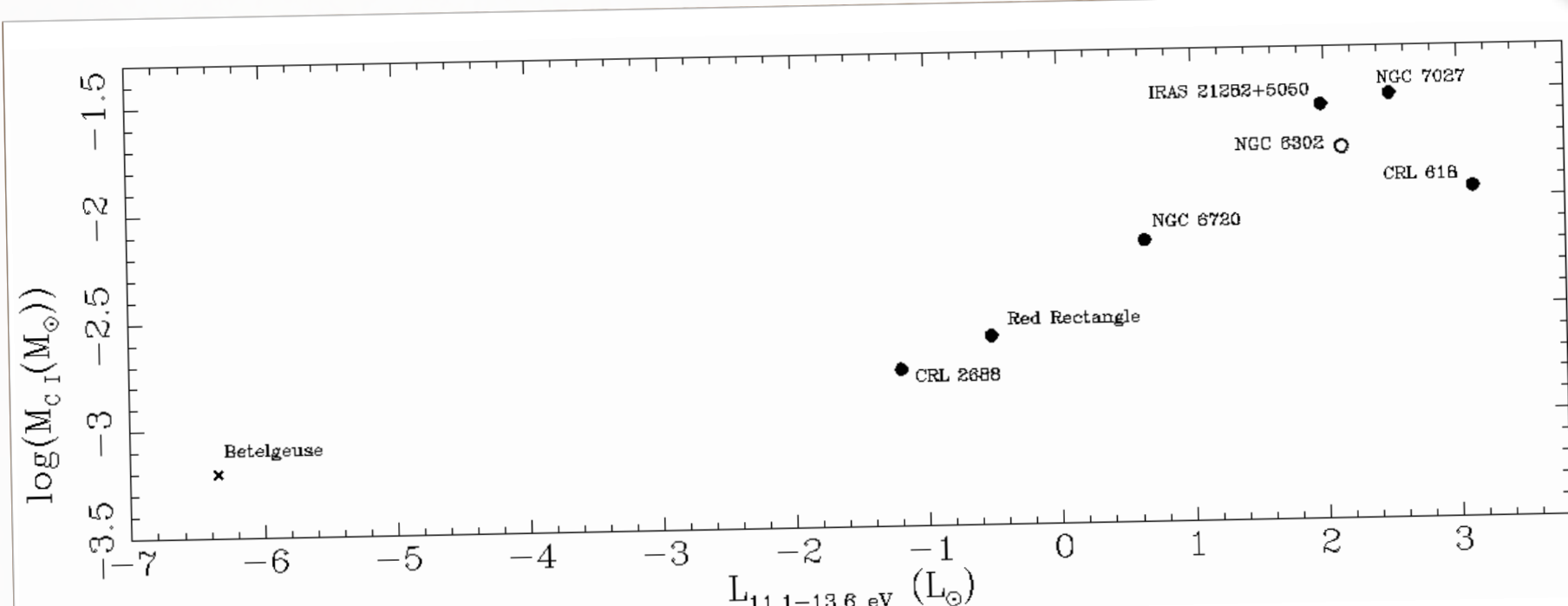


Figure 3. Mass of the C I-rich region against the CO photodissociation-capable luminosity of the central star.

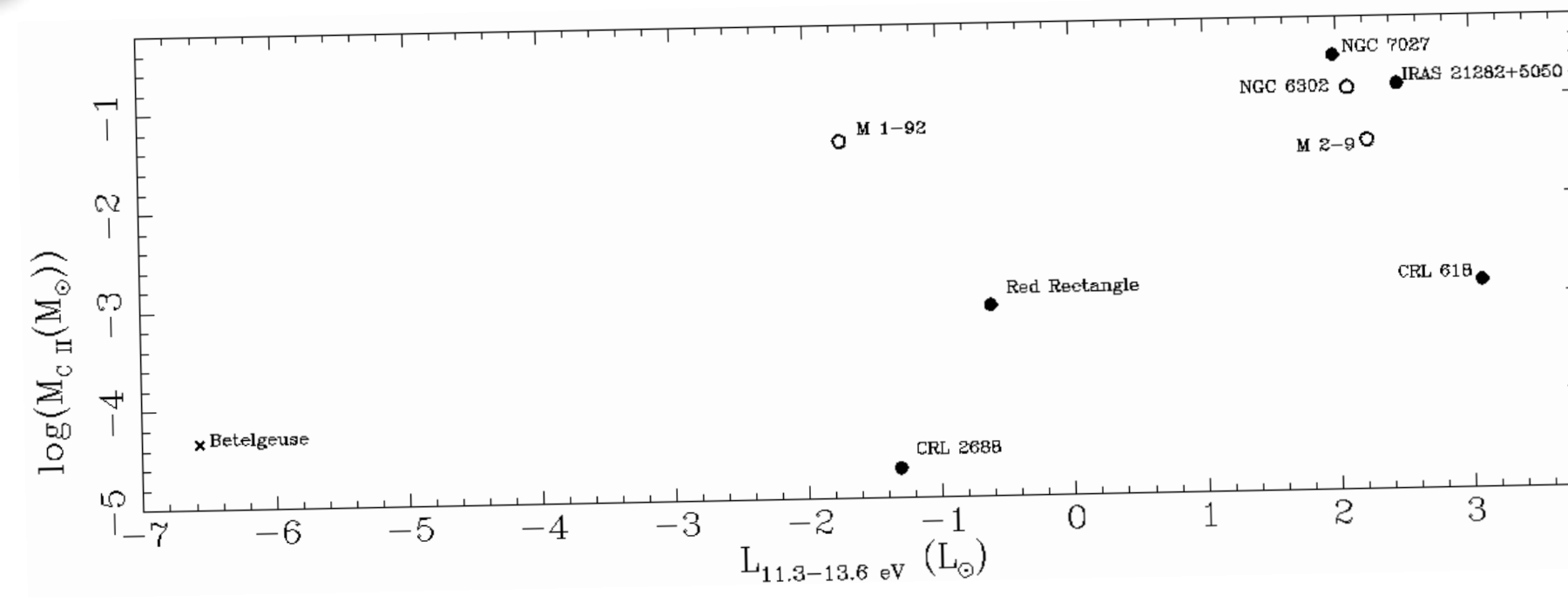


Figure 4. Mass of the C II-rich region against the C photoionization-capable luminosity of the central star.

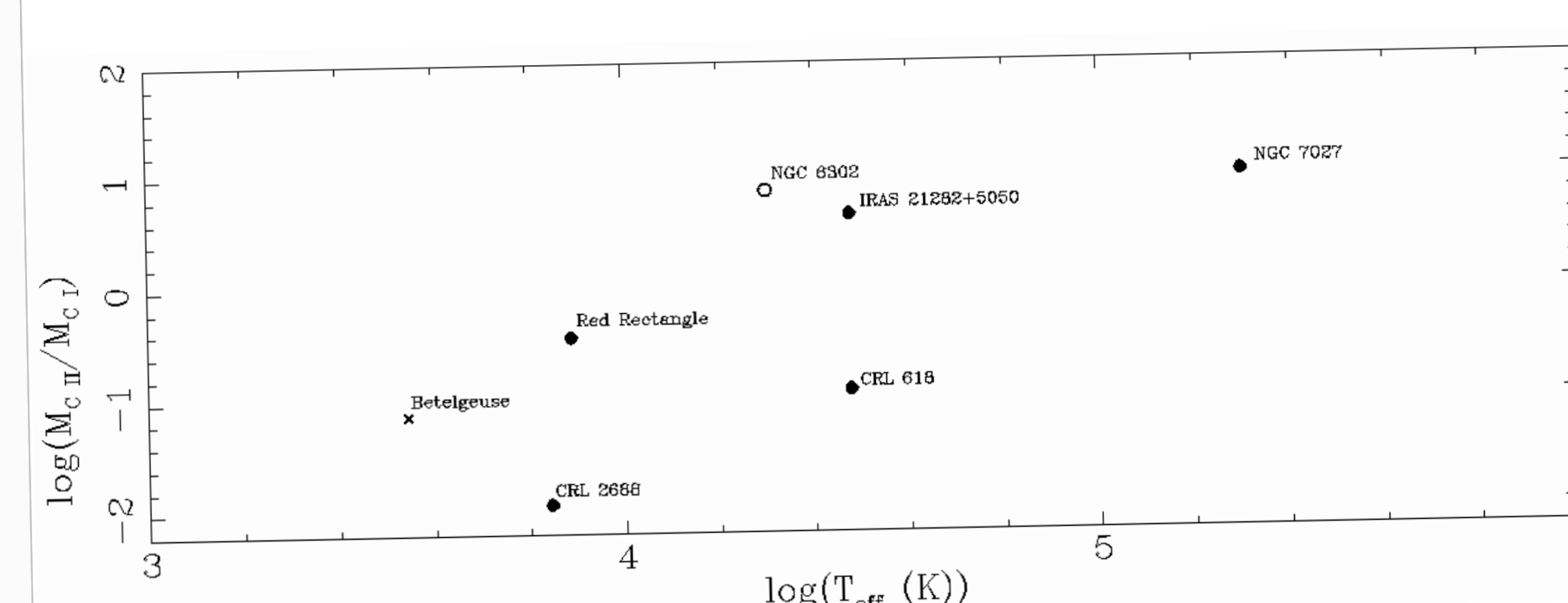


Figure 5. C II/C I mass ratio against the T_{eff} of the central star.

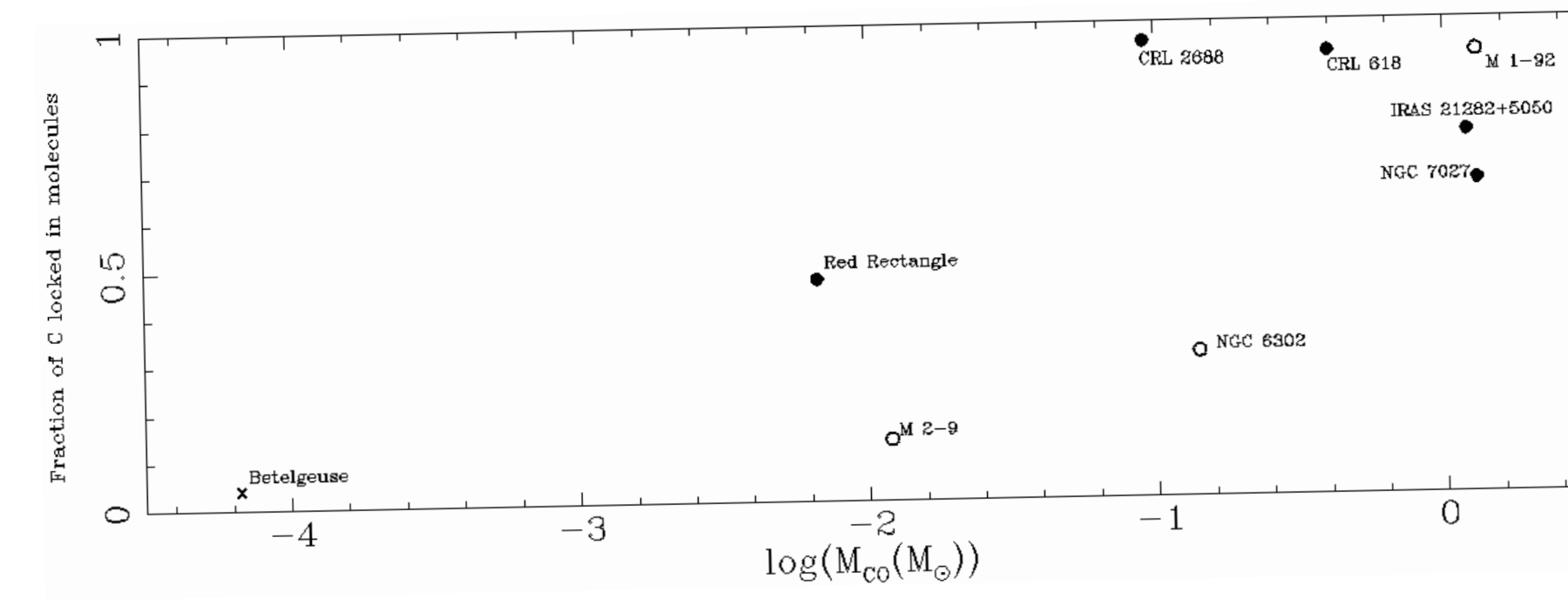


Figure 6. Fraction of carbon locked in molecules against the mass of the molecular envelope.

Preliminary conclusions

Figure 3 shows the logarithmic C I-rich region mass against the luminosity of the central star in the window 11.09-13.6 eV, whose photons can photodissociate CO from the inner edge of the molecular envelope and produce atomic carbon. With the exception of Betelgeuse, which has no PDR, there is a clear trend which confirms that atomic carbon is mainly located in a thin shell in the PDR. Also, C I seems to be produced by photodissociation rather than from shocks.

Figure 4 shows the logarithmic C II-rich region mass against the luminosity of the central star in the window 11.26-13.6 eV, whose photons can ionize neutral carbon. Again, a slight trend is present with a steeper slope than in the previous case. In general, the C II-rich region is more developed and massive, specially in objects with hot central stars. M 1-92 deviates from this trend; the fact that the C II line profiles are dominated by fast expansion supports the hypothesis of shock-induced C II production (e.g. Hollenbach & McKee 1989, ApJ, 342, 306). A clear trend can also be observed in Figure 5 showing the C II to C I mass ratio against T_{eff} of the central star.

These C I-rich and C II-rich region estimates, together with the mass of the molecular envelope derived from the literature allow us to establish other trends such as that in Figure 6, showing the fraction of carbon locked in molecules (as opposed to neutral or ionized atomic carbon) against the logarithmic mass of the molecular envelope. This shows that the most massive envelopes provide good shielding against the UV field of the star, therefore making molecule dissociation hard.